Supporting Information

Rational design and synthesis of SiC/TiC@SiO_x/TiO_2 porous core-shell nanostructure with excellent Li-ion storage performance

Chenyang Li[a], Jiaqian Qin[b*], Montree Sawangphruk[c], Xinyu Zhang[a*], and Riping Liu[a]

[a]*State Key Laboratory of Metastable Materials Science and Technology, Yanshan University, Qinhuangdao 066004, P. R. China*

[b] *Research Unit of Advanced Materials for Energy Storage, Metallurgy and Materials Science Research Institute, Chulalongkorn University, Bangkok 10330, Thailand*

[c]*Department of Chemical and Biomolecular Engineering, School of Energy Science and Engineering, Vidyasirimedhi Institute of Science and Technology, Rayong 21210, Thailand*

Experimental Section

Synthesis of Ti_3SiC_2. Starting powders of Ti (<45 μm, 99.5%), Si (1 μm, 99.9%), and TiC (3 μm, 99.9%) with the molar ratio of 2:2:3 were mixed in ethanol by agate mortar for 3 h, and then dried in vacuum. These powders were filled in a graphite die of 30 mm in diameter and sintered in vacuum by spark plasma sintering (SPS) at 1300 ℃ for 60 min. The heating rate was a constant of 50 ℃/min, and the applied pressure was controlled at 50 MPa.

Ball Milling Ti_3SiC_2. The as-prepared Ti_3SiC_2 was ball milled with the speed of 600 rpm for 15 h. And the weight ratio of the balls to powder was 10:1. Then the obtained powder was dispersed in deionized water, and then ultrasound 4 h. Subsequently, the solution was stilled in 12 h and centrifuged at 2000 rpm for 3 min to remove the large particles. Finally, the supernatant was centrifuged at 9500 rpm for 30 min, then dried in vacuum at 80 ℃. We named this prepared powder as TSC-15.

Oxidation treatment. 0.25 g TSC-15 was oxidized in muffle furnace at 350 ℃, 400 ℃, 450 ℃ for 60 min and 400 ℃ for 90 min, donated as TSC-15-350-60, TSC-15-400-60, TSC-15-450-60, and TSC-15-400-90, respectively.

Material Characterization

The X-ray diffraction (XRD, D\MAX 2500) was operated at 40 kV and 200 mA with a scanning speed of 2 °/min from 5° to 80°, to characterize the phase composition. The microstructure and morphology were analyzed by scanning electron microscopy (SEM, S4800) and transmission electron microscopy (TEM, JEM-2100F). The banding energy was studied by X-ray photoelectron spectroscopy (XPS, ESCALAB 250Xi). The specific surface areas and pore distribution were conducted on ASAP 2020 HD88, using the Brunaure-Emmet-Teller (BET) and Barrett-Joyner-Halenda (BJH).

Electrochemical Measurements. The as-prepared material, acetylene black and polyvinylidene fluoride (PVDF) were mixed in 1-methyl-2-pyrrolidinone (NMP) with a weight ratio of 70:15:15. 1M LiPF6 in a mixture of ethylene carbonate (EC) and dimethyl carbonate (DMC) (1:1 v/v%) was selected as the electrolyte. The

galvanostatic charge-discharge tests were performed on CT-4008 Battery Testing System at 16 ℃ with a voltage window of 0.02 to 3 V. Cyclic voltammetry (CV) measurements were conducted on CHI660E in the voltage range of 3-0.02 V (versus Li/Li+). Electrochemical impedance spectroscopy (EIS) was tested in a frequency range from 100 kHz to 0.1 Hz.

XPS analysis

To evaluate the chemical state and valence band information on the surface, X-ray photoelectron spectroscopy (XPS) is performed. The high-resolution XPS spectra of Ti 2p for TSC-15-350-60 (ESI†, Fig. S3a) is fitted into two peaks located at 458.79 and 464.49 eV, corresponding to Ti-O ($2p_{3/2}$) and Ti-O ($2p_{1/2}$), respectively, which is associated with TiO_2.[1] With the increase of the oxidation temperature and time, the Ti 2p peaks shift to the lower banding energy, which may be attributed to the increase of Ti^{3+} defects and oxygen vacancies.[2, 3] When the temperature reaches to 450℃, the peaks of Ti 2p move toward higher energy (458.84 and 464.54 eV), this probably owing to the formation of adjacent oxygen vacancies exhibiting a high electron-attracting effect.[4] Above all, no peaks appear in 454.40 eV corresponding to Ti-C, suggesting the titanium carbon compounds on the surface are totally oxidized. The Si 2p has one peak, as shown in Fig. S3b (ESI†), which is assigned to the Si-O bond. The peaks of C 1s (ESI†, Fig. S3c) are centered at 284.77, 286.37, 288.91 eV, which could be assigned to C-C, C-O and C=O.[5] Similarly, no peak can be detected at 281.00 eV, implying Ti-C bond does not exist, which is accord with the result of Ti 2p. As shown in Fig. S3d (ESI†), the O 1s has four peaks at 530.24, 531.20, 532.11 and 533.00 eV, which are ascribed to Ti-O, C-O,[6] oxygen vacancies[7] and Si-O. The XPS results father confirm that the shell is consisted with TiO_2 and SiO_x.

EIS analysis

To further understand the charge transfer kinetics of TSC-15-400-90, the electrochemical impedance spectroscopy (EIS) is conducted. In Fig. S6a (ESI†), the Nyquist plot consists of a semicircle in the high-medium frequency region and an incline line in the low frequency region. Before cycling, the semicircle of TSC-15-400-90 is the smallest, indicating the smallest charge-transfer resistance (R_{ct}).[8] After 200 cycles, another semicircle appears (ESI†, Fig. S6b) suggesting the formation of SEI film.[9]

After 200 cycles, the XPS results of TSC-15-400-90 can be seen in Fig. S6c-f, the peaks of Ti 2p and Si 2p just shift toward the lower banging energy, indicating the Li^+ embed in the TiO_2 and SiO_x crystal lattices. The new peaks of C1s at 289.65 eV and O 1s at 531.71 eV represent the Li_2CO_3, and the peaks of C1s at 290.56 eV and O 1s at 533.26 eV corresponding to the C-F bond and O-F bond, respectively. The existence of Li_2Co_3, C-F bond and O-F bond illustrate the formation of SEI film, which is identical with the results of EIS.

Table S1. The BET results and shell thickness of TSC-15-350-60, TSC-15-400-60, TSC-15-400-90 and TSC-15-450-60.

Sample	BET Surface Area (m^2/g)	Average Pore Diameter (nm)	Pore Volume (cm^3/g)	Shell Thickness (nm)
TSC-15-350-60	10.57	7.1	0.022	40
TSC-15-400-60	15.65	6.7	0.030	100
TSC-15-400-90	26.41	6.4	0.051	130
TSC-15-450-60	29.29	6.0	0.043	Completely Oxidized

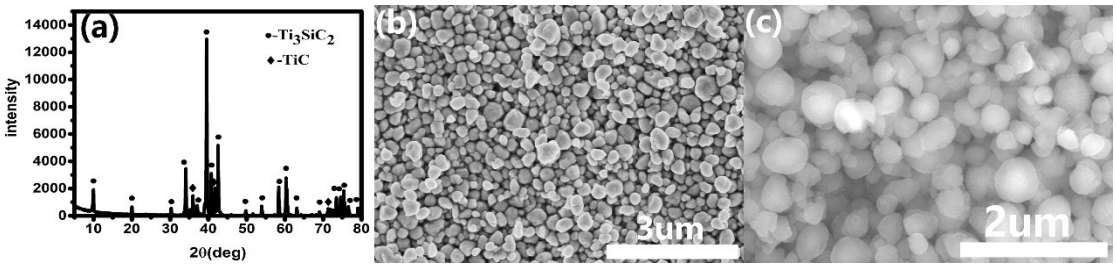

Figure S1. a) XRD pattern of Ti_3SiC_2. b) SEM image of TSC-15. c) SEM image of SiC/TiC@SiO_x/TiO_2.

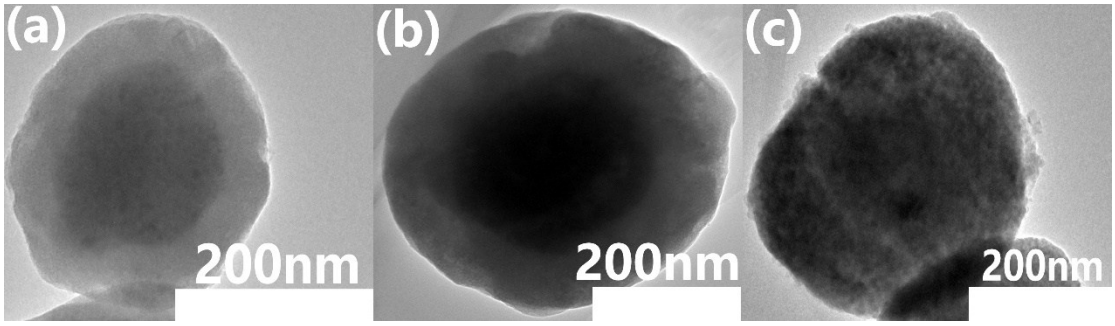

Figure S2. TEM image of a) TSC-15-350-60, b) TSC-15-400-60 and c) TSC-15-450-60.

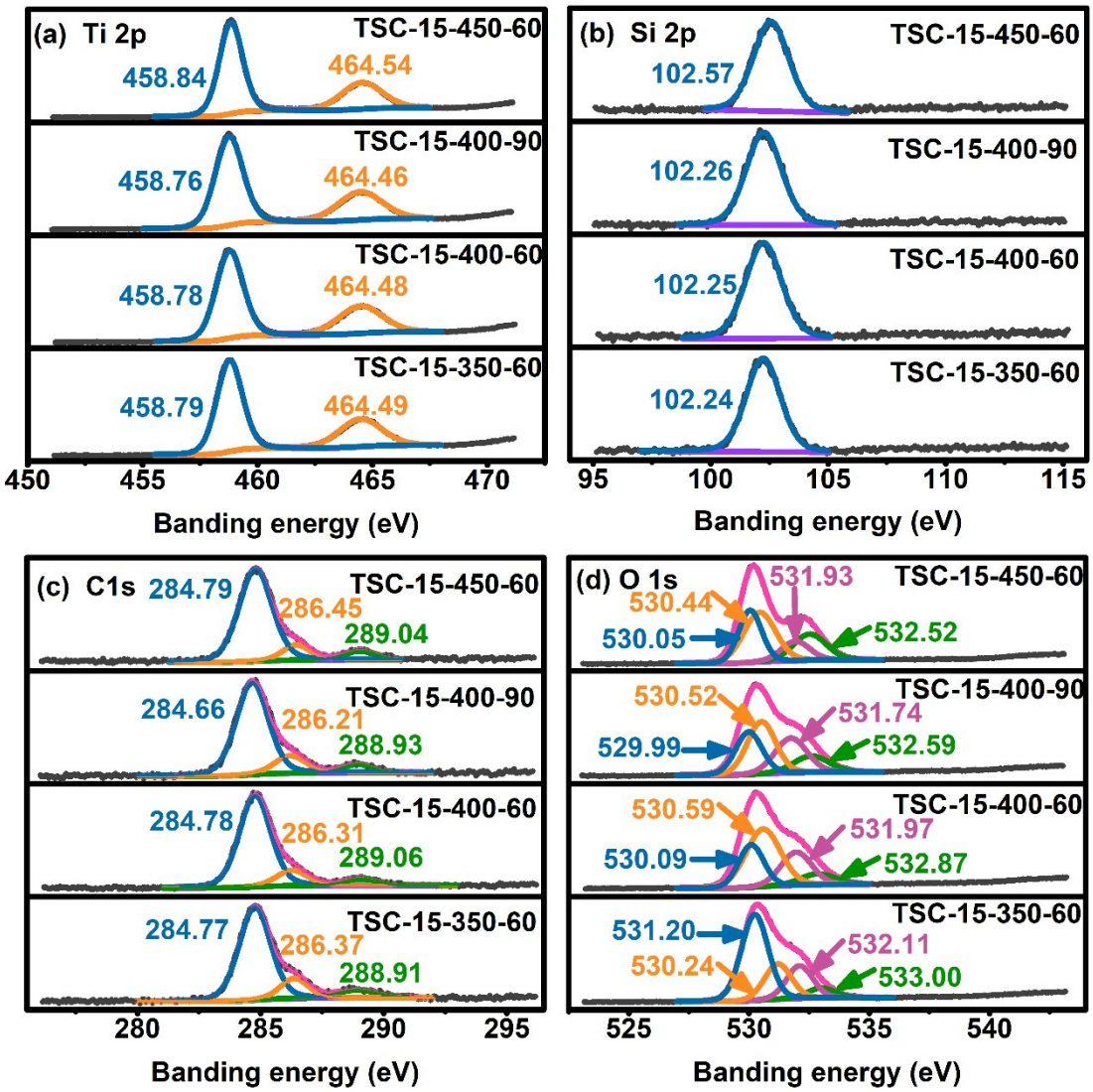

Figure S3. High-resolution XPS spectra of a) Ti 2p, b) Si 2p, c) C 1s and d) O 1s of TSC-15-350-60, TSC-15-400-60, TSC-15-400-90 and TSC-15-450-60.

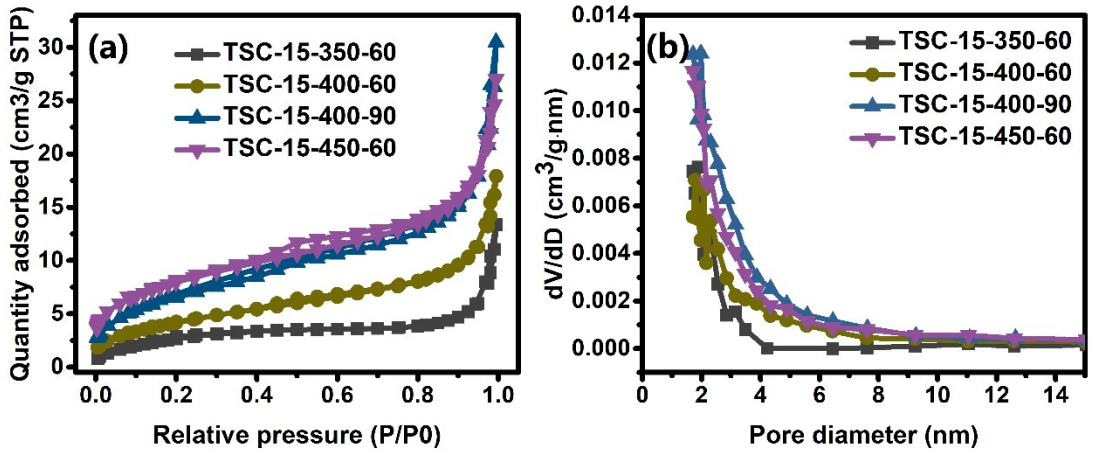

Figure S4. a) N_2 adsorption-desorption isotherms curves and b) pore size distribution of TSC-15-350-60, TSC-15-400-60, TSC-15-400-90 and TSC-15-450-60.

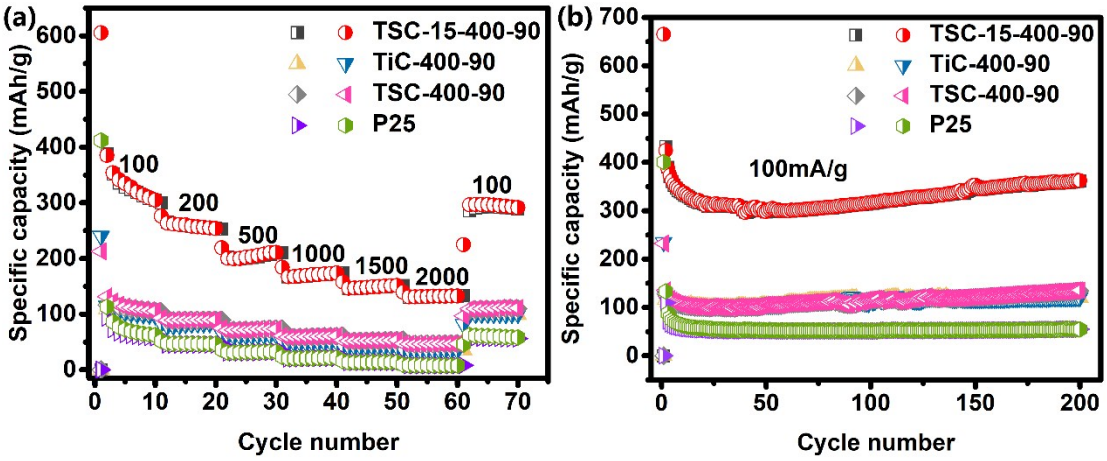

Figure S5. a) Cycling performance and b) rate performance of TSC-15-400-90, TiC-400-90, TSC-400-90 and P25.

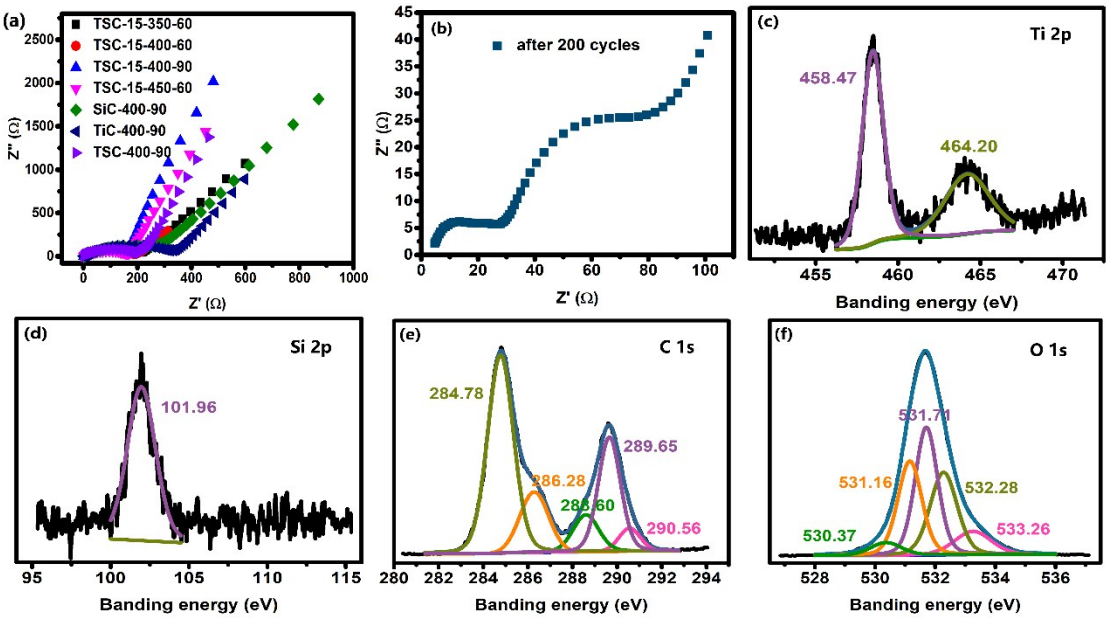

Figure S6. a) Electrochemical impedance spectra of all heat-treatment samples. b) Nyquist plots after 200 cycles. c) XPS spectra of c) Ti 2p, d) Si 2p, e) C 1s and f) O 1s of TSC-15-400-90 after 200 cycles.

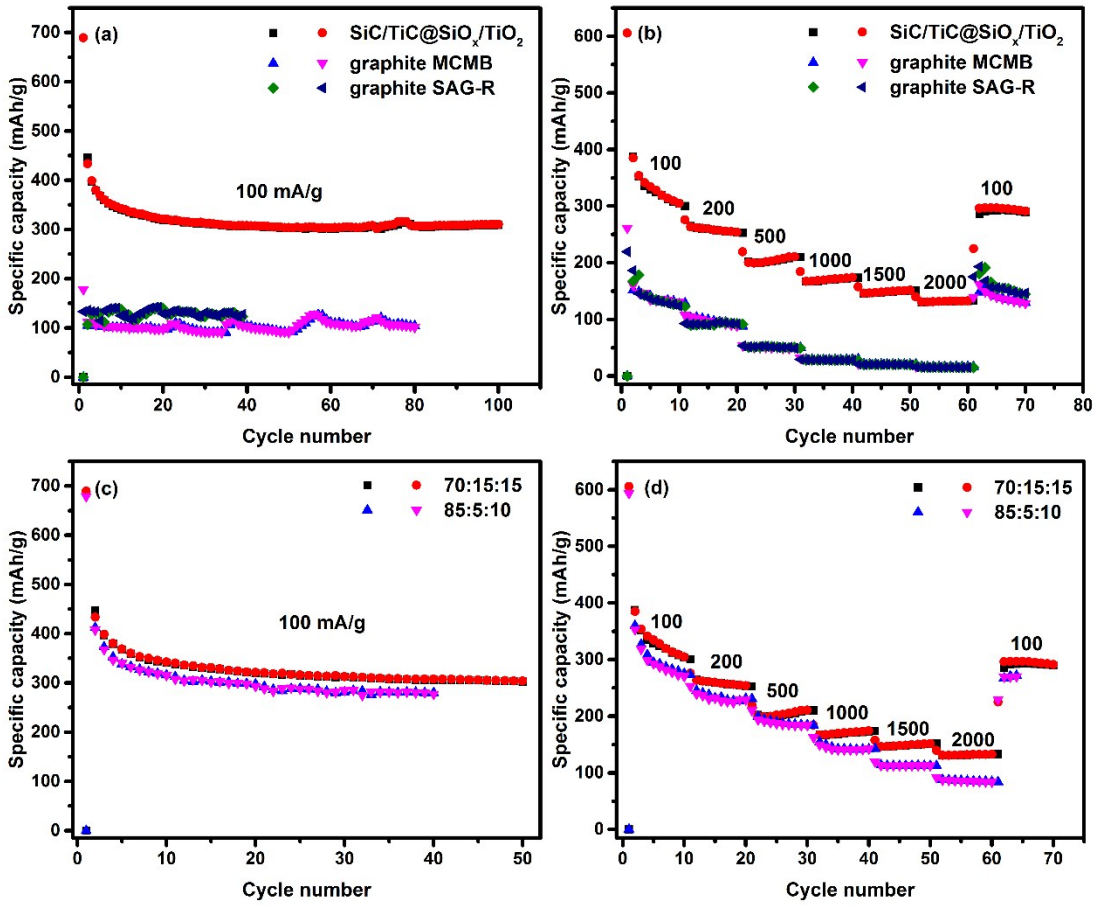

FigureS7. a) Rate performance of SiC/TiC@SiO_x/TiO_2, MCMA and SAG-R, at 100, 200, 500, 1000, 1500, 2000 and 100 mA/g. b) Cycling behavior of SiC/TiC@SiO_x/TiO_2, MCMA and SAG-R at 100 mA/g. c) Rate comparison of active material with different proportions. d) Cycling performance of active material with different proportions.

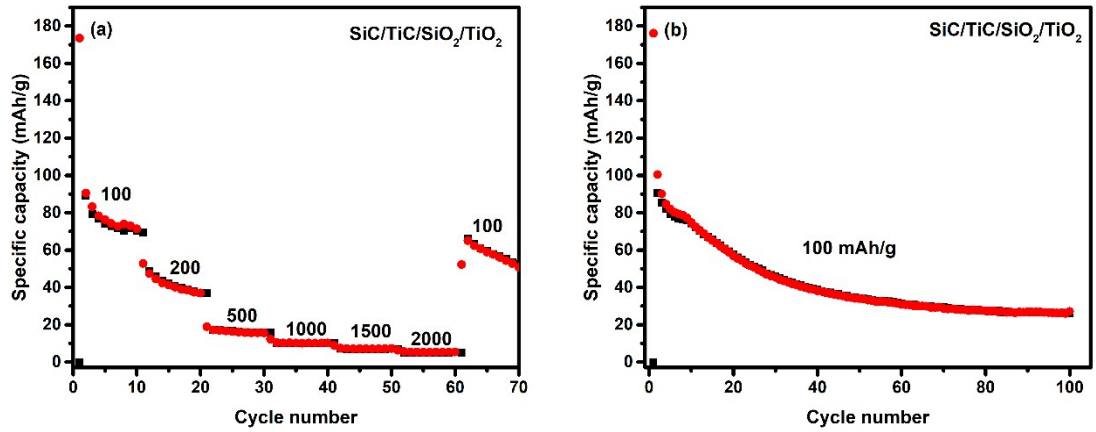

FigureS8. a) Rate performance of SiC/TiC/SiO_2/TiO_2. b) Cycling behavior of SiC/TiC/SiO_2/TiO_2.

Supporting references

1. L. Zhang, M. S. Tse, O. K. Tan, Y. X. Wang and M. Han, *J Mater Chem A*, 2013, **1**, 4497-4507.
2. Y.-F. Lee, K.-H. Chang, C.-C. Hu and K.-M. Lin, *J Mater Chem*, 2010, **20**, 5682-5688.
3. C. Yang, X. Zhang, J. Qin, X. Shen, R. Yu, M. Ma and R. Liu, *J Catal*, 2017, **347**, 36-44.
4. M. Xing, J. Zhang, F. Chen and B. Tian, *Chem Commun (Camb)*, 2011, **47**, 4947-4949.
5. D. H. Wang, L. Jia, X. L. Wu, L. Q. Lu and A. W. Xu, *Nanoscale*, 2012, **4**, 576-584.
6. L.-C. Chen, Y.-C. Ho, W.-S. Guo, C.-M. Huang and T.-C. Pan, *Electrochim Acta*, 2009, **54**, 3884-3891.
7. Z. Jin, H. Gao and L. Hu, *RSC Adv*, 2015, **5**, 88520-88528.
8. X. Guo, X. Xie, S. Choi, Y. Zhao, H. Liu, C. Wang, S. Chang and G. Wang, *J Mater Chem A*, 2017, **5**, 12445-12452.
9. N. Chen, Y. Yao, D. X. Wang, Y. J. Wei, X. F. Bie, C. Z. Wang, G. Chen and F. Du, *ACS Appl Mat Interfaces*, 2014, **6**, 10661-10666.